Oxidative Coupling of Methane on Improved Bismuth Oxide Membrane Reactors

Y. Zeng and Y. S. Lin
Dept. of Chemical Engineering, University of Cincinnati, Cincinnati, OH 45221

Fluorite-structured yttria-bismuth oxide membranes with improved chemical stability were prepared by doping samarium in the lattice. The samarium-doped yttria-bismuth oxide (BYS) membranes are in fluorite structure, with high oxygen permeability and good catalytic properties for oxidative coupling of methane (OCM). The oxygen partial pressure dependence of oxygen permeation flux shows a shift of the rate-limiting step from the surface reaction to the bulk electron-hole conduction as temperature increases from 750 to 950°C. OCM reactions were conducted in a membrane reactor made of the disk-shaped BYS membrane. Methane- and oxygen-containing streams are fed into the opposite sides of the BYS membrane to allow OCM reactions to occur on the membrane surface exposed to methane. The membrane reactor gives C_2 yields of 4–11% with C_2 selectivity up to 74%. The performance of this membrane reactor is closely related to oxygen permeation properties of the BYS membrane. Experimental results show the effectiveness in improving the C_2 yield by increasing the membrane surface area to reactor volume ratio. In this disk-shaped membrane reactor the highest C_2 yield achieved is 17%, with a C_2 selectivity of about 80%.

Introduction

Oxidative coupling of methane (OCM) is a promising process for direct conversion of natural gas (90% of methane) into more useful C_2 (C_2H_4 and C_2H_6) products (Fox, 1993). Extensive research on catalysis for OCM was reported in the 1980s. Due to undesired gas-phase combustion reactions, the C_2 yields achieved so far over any solid oxide catalysts operated in a conventional packed-bed reactor are less than 30% if the C_2 selectivity is maintained higher than 50%. Since the early 1990s, studies on OCM have been shifted from finding better catalysts to developing new reactor configurations that fit better the OCM reaction mechanism and kinetics than the conventional packed-bed one (Tonkovich et al., 1993; Tonkovich and Carr, 1994; Jiang et al., 1994). Although the overall C_2 yield of higher than 30% has been achieved in these reactors, the C_2 yield per path is still much lower than 30%.

Membrane reactors have traditionally been studied as a means of improving the yield of the reactions of limited conversion by removing one of the products from the reactor. OCM represents another group of chemical reactions with a selectivity, not conversion, problem. Membrane reactors for OCM have recently received increasing attention because of the fundamental and practical significance of such membrane reactor processes. By regulating reactant streams, porous (Lafarga et al., 1994; Coronas et al., 1994; Ramachandra et al., 1996; Tonkovich et al., 1996; Lu et al., 1997) and dense (Kao et al., 1997; Lu et al., 2000) ceramic membrane reactors packed with an OCM catalyst have the potential to kinetically improve the C_2 selectivity and yield of OCM. Dense ionic-conducting ceramic membrane can also be used to improve mechanistically the C_2 selectivity and OCM yield by allowing OCM to react with the active oxygen on the membrane surface (Nozaki et al., 1992, 1993; Nozaki and Fujimoto, 1994; ten Elshof et al., 1995; Wang and Lin, 1995; Xu and Thomson, 1997; Zeng et al., 1998). These dense membrane reactors, if consisting of a membrane with high oxygen permeability and good intrinsic OCM catalytic properties, are promising for achieving high C_2 selectivity and yield for OCM.

In OCM, oxygen ions on the oxide catalyst surface promote the generation of C_2 products, while gas-phase oxygen

---

Correspondence concerning this article should be addressed to Y. S. Lin.

molecules favor the formation of CO_x (Ito et al., 1985). In the dense ionic-conducting ceramic membrane reactor, methane and oxygen (or air) are respectively introduced to the opposite sides of the membrane wall. Oxygen permeates through a dense oxygen-conducting ceramic membrane at high temperature under an oxygen partial pressure gradient (Bouwmeester et al., 1992; Bouwmeester and Burggraaf, 1996). The oxygen ions move through the membrane wall and react with methane on the membrane surface exposed to the methane stream. If the membrane surface itself (uncoated with other OCM catalyst material) has good catalytic properties (in terms of both activity and selectivity) for formation of methyl radicals, and the supply of the oxygen ions matches the conversion of methane to C_2 products, it is possible to obtain high C_2 yields for OCM in these dense ceramic membrane reactors (Wang and Lin, 1995).

Perovskite-type lanthanum cobaltite ceramic membranes have good oxygen permeability. But they do not offer good catalytic properties for OCM, especially under reducing conditions (Lin and Zeng, 1996). As a result, OCM reactions on the perovskite-type ceramic membranes do not show much improvement in the C_2 yield and selectivity (ten Elshof et al., 1995; Zeng et al., 1998). In contrast, the fluorite-type bismuth-oxide-based ceramics (such as 25 mol % Y_2O_3 doped Bi_2O_3, abbreviated as BY25) are good oxygen ionic conductors and have excellent OCM catalytic properties (Zeng and Lin, 1997a), even under the reducing atmosphere (Zeng and Lin, 1997b). The BY25 membranes showed a considerably high oxygen permeability at temperatures above 800°C (Zeng and Lin, 2000b). The C_2 selectivity for OCM in the membrane reactor made of a disk-shaped BY25 membrane is about 30% higher than that in the cofeed fixed-bed reactor packed with the same BY25 pellets under the conditions that give the similar C_2 yield. C_2 yields as high as 16% were obtained in the disk-shaped BY25 membrane reactor. This is the highest C_2 yield reported on the disk-shaped dense ceramic membranes for OCM.

It is known that bismuth oxide is not chemically stable under reducing conditions. In the previous work the BY25 membrane disk remained in good mechanical integrity after OCM experiments but some impurity phases were found on the membrane surface exposed to the methane stream (Zeng and Lin, 2000b). It is expected that the BY25 membrane will experience a considerable phase structure change after prolonged exposure to methane under the OCM reactions. In order to stabilize its fluorite-type phase structure under reducing environment and at high temperatures, samarium oxide was doped into the BY oxide to form an improved Bi_2O_3-based oxygen-ionic conducting material with a formula of $Bi_{1.5}Y_{0.3}Sm_{0.2}O_3$. The selection of samarium as the dopant was based on the considerations that (1) samarium oxide is known for its good OCM catalytic properties; (2) it has a higher melting point than bismuth oxide; and (3) it may enhance electronic conductivity of the membrane due to the occurrence of both Sm^{2+} and Sm^{3+}.

The improvement in the stability of the bismuth-oxide-based membranes not only is important from the view point of practical applications but also allowed us to perform more time-consuming OCM experiments on each of the membrane sample to provide better insights into the new membrane reactor. The present article reports results of oxygen permeation measurements and OCM reactions in the BYS membrane reactor.

Experimental Studies

The powders of $Bi_{1.5}Y_{0.3}Sm_{0.2}O_3$ (abbreviated as BYS) were synthesized by the citrate method described in detail elsewhere (Zeng and Lin, 2000a). In brief, the preparation procedure includes: (1) polymerization reactions between citric acid and the corresponding metal nitrates in an aqueous solution; (2) condensation reactions among the aforementioned polymeric compounds to form a gel-like material; (3) self-ignition reactions of the just-mentioned dried gel in an oven at about 400°C; (4) calcination of the charred materials formed in step (3) at 750°C for 3 h. The powder was then packed in a stainless-steel cylindrical mold and uniaxially pressed into a disk shape. The disks were then sintered at 1050°C for 48 h to a relative density of higher than 95%. The BYS membrane disks used in this work were 1.27 mm in thickness and 21 mm in diameter. The phase structure of the membranes was examined by X-ray diffraction (Siemens Kristalloflex D500 diffractometer, with Cu Kα radiation). Their gas tightness at room temperature was confirmed by helium permeation.

Oxygen permeation and OCM experiments were performed on a high-temperature permeation/reactor system with the GC analysis method described in detail in a previous publication (Zeng et al., 1998). Figure 1a shows the schematic of the central part of the reactor. The membrane disk was sealed with a sealing material consisting of a glass and BYS powder on the top of a vertically placed 1-in.-OD (25 mm) dense α-Al_2O_3 tube which was coaxially inserted inside a 1.5-in.-OD (38 mm) dense α-Al_2O_3 tube. During OCM or oxygen permeation experiments, a 1:1 O_2/N_2 gas mixture was introduced through a 1/4-in.-OD (6 mm) dense α-Al_2O_3 tube into the chamber inside the 1-in.-OD (25 mm) tube (referred to as the upstream or oxygen chamber) and led over one side of the membrane disk. A 10% methane/helium mixture (for OCM reaction) or pure He (purity 99.99%) (for oxygen permeation) passed through another 1/4-in.-OD dense α-Al_2O_3 tube into the chamber within the 1.5-in.-OD alumina tube (referred to as the downstream or reaction chamber) and flushed over the other side of the membrane disk. As with most experimental studies reported on OCM, methane with a diluent (helium), instead of pure methane, was used as the feed in this work in order to avoid the excessive reaction heat generated during reaction. The flow rates in the up- and downstream chambers were controlled at, respectively, 50 mL/min and 100 mL (for oxygen permeation) or 50–200 mL (for OCM reaction) by mass flow controllers.

The effluent from the downstream (reaction) chamber was intermittently sampled by a 10-port rotary valve (Valco Instruments), and analyzed by a GC that could detect oxygen with a concentration as low as 200 ppm. Oxygen concentrations in both the up- and downstream chambers were also monitored by a yttria-stabilized zirconia oxygen sensor (6000 Oxygen Analyzer, from Illinois Instruments). Gas leakage through the sealant, if it occurred, could be detected by monitoring nitrogen concentration in the downstream chamber. Oxygen permeation flux was calculated from the flow rate and oxygen molar fraction of the downstream effluent.

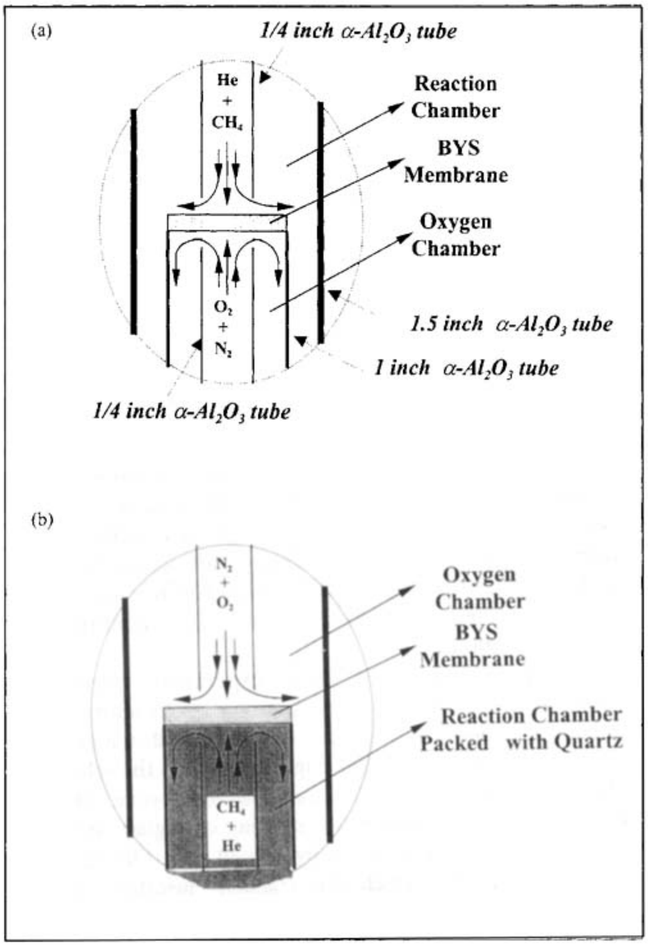

Figure 1. (a) Central part of the membrane reactor and flow configuration; (b) that of a modified flow configuration with increased membrane surface area to reaction volume.

OCM reactions were also performed in the same membrane reactor, with the feeds of O_2/N_2 and CH_4/He reversed, as shown in Figure 1b. In this case the 1-in.-OD dense α-alumina tube was packed with 1 mm quartz particles to reduce the gas-phase volume of the reaction chamber. For OCM in both reactor configurations shown in Figures 1a and 1b, the composition of reaction chamber effluent was analyzed by GC and the methane conversion was calculated by

$$C = \left(Q_{\text{in}} X_{\text{CH}_4} - Q_{\text{out}} Y_{\text{CH}_4}\right) / Q_{\text{in}} X_{\text{CH}_4}, \qquad (1)$$

where Q stands for the volumetric flow rate, and X and Y are molar fractions in the feed and effluent of the reaction chamber, respectively. The selectivity for the carbon-containing product i is the percentage of reacted methane that forms product i and was calculated by

$$Si = \left(Q_{\text{out}} n_i Y_i\right) / \left(Q_{\text{in}} X_{\text{CH}_4} - Q_{\text{out}} Y_{\text{CH}_4}\right), \qquad (2)$$

where n_i is the number of carbon atoms in the molecule of the carbon-containing product i. The C_2 yield is the percentage of total methane that forms ethane and ethylene, which was calculated from the product of methane conversion and C_2 selectivity.

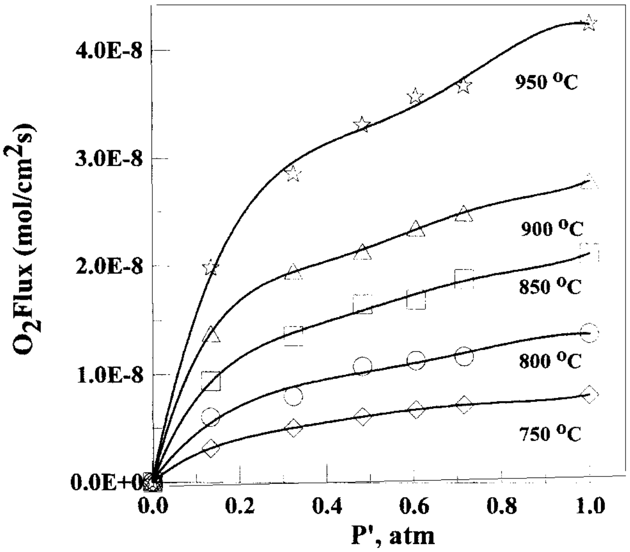

Figure 2. Oxygen permeation through BYS membrane as function of oxygen partial pressure.

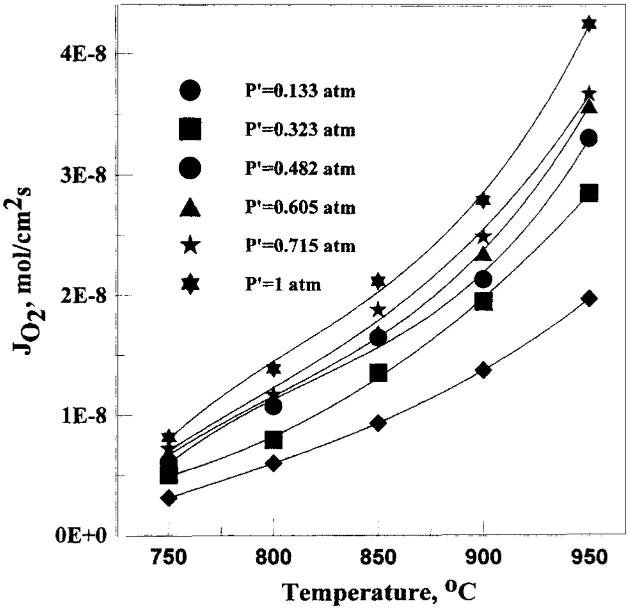

Figure 3. Oxygen permeation flux through BYS membrane as function of temperature.

Results and Discussion

Figure 2 gives oxygen permeation fluxes through a BYS membrane as a function of upstream oxygen partial pressure at various temperatures from 750°C to 950°C. The temperature dependence of the oxygen permeation flux at different oxygen partial pressures is shown in Figure 3. The oxygen permeation flux can be correlated to the up- and downstream

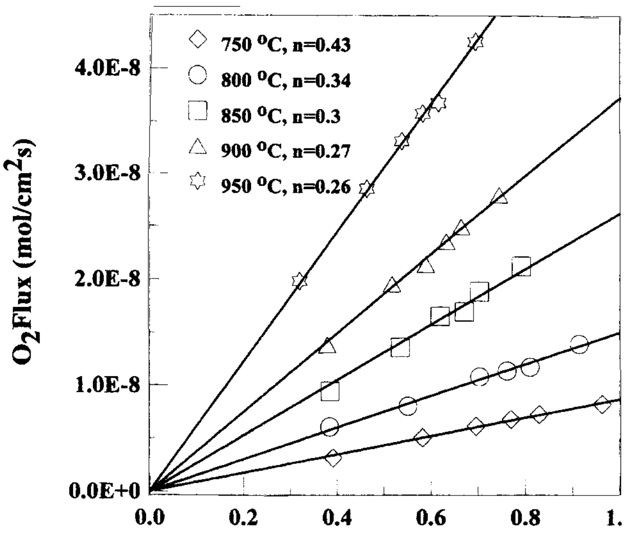

Figure 4. Regression of oxygen permeation flux data at different oxygen partial pressures by Eq. 3.

oxygen partial pressures, P' and P'', by the following empirical equation (Lin et al., 1994; Bouwmeester and Burggraaf, 1996)

$$J_{O_2} = k(P'^n - P''^n), \tag{3}$$

where the values of k and n are, respectively, the lumped rate constant and kinetic order with respect to oxygen partial pressure. Figure 4 gives the plots of J_{O_2} vs. $(P'^n - P''^n)$. These plots show straight lines through the original, indicating that Eq. 3 can be applied to describe the effects of oxygen partial pressure on the permeation flux. Table 1 lists the regressed values of k and n at different temperatures.

The values of k in Table 1 can be well correlated to temperature by the Arrhenius equation (with the regression coefficient $R^2 = 0.996$ by Microsoft Excel) to give the activation energy of 100.6 kJ/mol. The value of n decreases from 0.43 to 0.26 with increasing temperature from 750°C to 950°C. It is known that the oxygen permeation through bismuth-oxide-based ceramic membranes is determined by the rate steps of the surface reactions on both membrane surface and electron–hole conduction in the membrane bulk (Lin et al., 1994; Bouwmeester and Burggraaf, 1996). The value of n is 0.5 if the surface reactions are the rate limiting step, and 0.25 if the electronic conduction in the membrane bulk is rate limiting. The fact that the n value at 750°C is very close to 0.5 indicates that the surface reactions dominate the oxygen permeation at this temperature. At 950°C, the n value is close to 0.25, indicating bulk electron-conduction becomes the rate-limiting step at high temperature.

Table 1. Parameters in Eq. 3 at Different Temperatures

Temp. °C	750	800	850	900	950
k	8.65	15.0	26.2	37.3	61.4
n	0.43	0.34	0.30	0.27	0.26

Note: k in the unit of $[10^{-9}$ mol/cm$^2\cdot$s$\cdot$atm$^n]$.

The preceding results show that the rate-limiting step changes from the surface reactions to the bulk conduction as temperature increases from 750°C to 950°C. This suggests that surface reaction steps require higher activation energy than the bulk electronic conduction in the BYS membrane, consistent with the activation energy data for oxygen permeation through erbia-stabilized bismuth oxide (184 kJ/mol for the surface reaction and 54.6 kJ for the bulk diffusion) (Lin et al., 1994). The activation energy of 100.6 kJ/mol obtained from the k values from Eq. 3 in the temperature range of 750–950°C should be considered as an apparent activation energy averaging those for the bulk electronic conduction and surface reactions for oxygen permeation through BYS membrane.

An oxygen permeation flux of 6.7×10^{-9} mol/cm$^2\cdot$s was reported for a 0.7-mm-thick 25 mol % Er_2O_3-Bi_2O_3 (BE25) membrane at 810°C with P' and P'' being, respectively, 1 and 1.1×10^{-4} atm (Bouwmeester et al., 1992). The oxygen permeation flux through the 1.27-mm-thick BYS membrane at 800°C under the same oxygen partial pressures is 1.43×10^{-8} mol/cm$^2\cdot$s, about two times that of the BE25 membrane, even without considering the effect of thickness. The oxygen permeation fluxes through the BYS membrane are similar to those through the BY25 membrane (Zeng and Lin, 2000b). This suggests that the dopant yttrium, not samarium, plays the major role in improving the electron-hole conductivity of the bismuth-oxide-based ceramics.

Upon introducing methane into the downstream chamber, methane starts to react with oxygen ions on the surface of the BYS membrane. Ethane and ethylene were thus generated. The oxygen ions on this surface were renewed by the transport of oxygen from the other side of the membrane. Gas-phase oxidation reactions could occur if oxygen was released from the membrane surface into the gas phase in the reaction chamber.

Figures 5 to 8 show the temperature dependence of methane conversion, C_2 selectivity and yield, and C_2H_4/C_2H_6 ratio in the product at several different methane/helium flow rates. The effects of the methane/helium flow rate on the results of OCM in the membrane reactor are complex. It appears that the methane conversion and C_2 yield are maximum at the flow rate of 150 mL/min in most parts of the temperature range studied. This could be due to the fact that the higher flow rate promotes the mass transport from solid phase to gas phase as well as in the gas phase itself. Methane conversion increases exponentially with increasing temperature for all flow rates. The shapes of the curves in Figure 5 (methane conversion vs. temperature) are very similar to those in Figure 3 (oxygen permeation flux vs. temperature), suggesting that the OCM reaction rate is enhanced by increasing oxygen permeation flux as temperature increases. Unlike the cofeed packed-bed reactor in which C_2 selectivity generally increases with increasing temperature, C_2 selectivity shown in Figure 6 increases and, after passing a maximum of 74% at around 800–850°C, decreases with increasing temperature.

At flow rates of 100 and 150 mL/min, the temperature dependence of C_2 yield shows a maximum at 850°C. The temperature effects on C_2 selectivity and yield in the BYS membrane reactor are related to the oxygen permeation

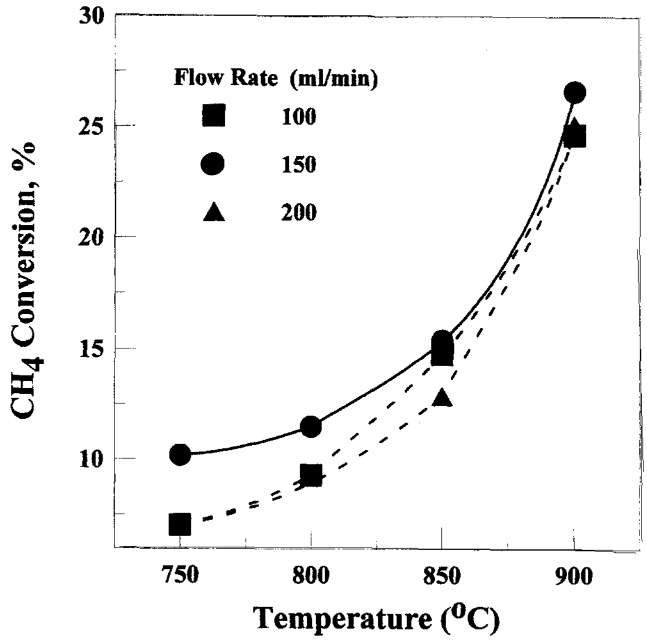

Figure 5. Methane conversion as a function of temperature in BYS membrane reactor.

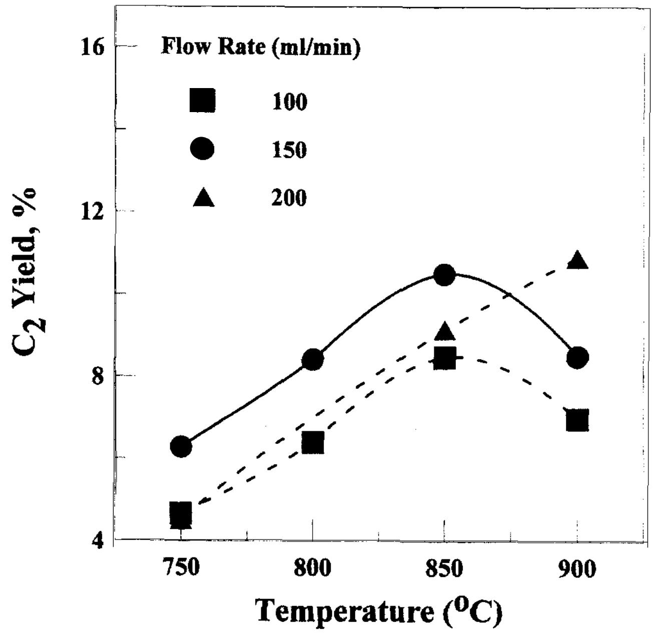

Figure 7. C_2 yield as a function of temperature in BYS membrane reactor.

properties of the BYS membrane. The active oxygen on the membrane surface exposed to methane is consumed by OCM and should be replenished with oxygen permeating from the other surface of the membrane. The C_2 selectivity and yield increase with temperature due to the fact that the availability of the surface-active oxygen, determined by the oxygen permeation rate, increases with temperature from 750°C to 850°C. However, if the oxygen permeation rate is larger than the oxygen consumption rate by OCM reactions, some of the oxygen permeating through the membrane wall would get into the gas phase, lowering the C_2 selectivity and yield due to gas-phase combustion reactions (Wang and Lin, 1995). This is why a further increase in temperature results in a decrease in both C_2 selectivity and yield.

Figure 8 shows that the C_2H_4/C_2H_6 ratio increases exponentially, from about 0.5 to 3.5, with increasing temperature.

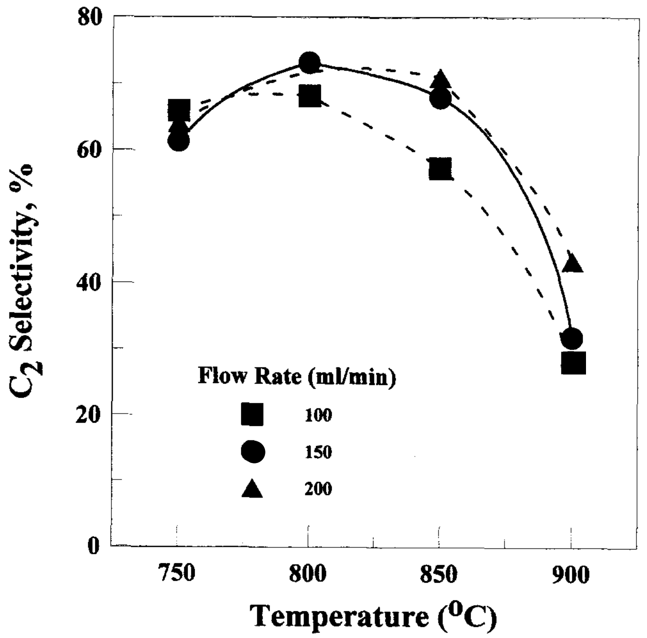

Figure 6. C_2 selectivity as a function of temperature in BYS membrane reactor.

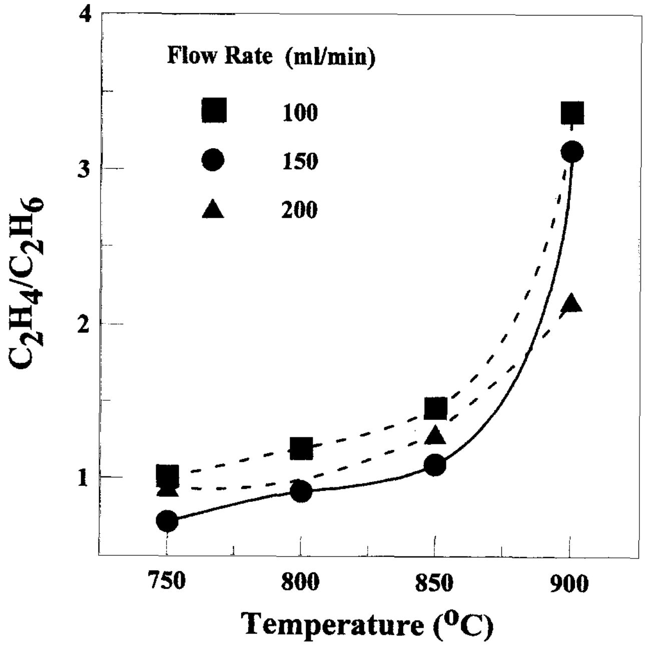

Figure 8. C_2H_4/C_2H_6 ratio in product as a function of temperature in BYS membrane reactor.

Similar to OCM in the cofeed packed-bed reactor, ethylene in the membrane reactor also comes from the dehydrogenation of ethane. However, the C_2H_4/C_2H_6 ratio in a cofeed reactor packed with BYS pellets under similar conditions increases from 0.5 to 2 as temperature increases from 800°C to 900°C. In the membrane reactor the formation of ethylene is more likely to take place on the membrane surface instead of in the gas phase as found in the packed-bed reactor, due to the absence of oxygen in the gas phase in the membrane reactor. Since the concentration of C_2H_6 is higher on (or near) the surface of the membrane than in the bulk gas phase, conversion of C_2H_6 to C_2H_4 is expected at a higher rate in the membrane reactor than in the cofeed reactor.

Oxygen permeation flux during OCM, estimated from the data of the flow rate, methane conversion, and selectivity, is about 1.5×10^{-7} mol/cm²·s at 800°C and methane/helium flow rate of 100 mL/min (10% methane). This value is about 10 times the oxygen permeation flux with helium as the purge gas in the downstream under similar conditions. This difference is partly due to the larger oxygen partial pressure gradient during OCM reaction ($P' = 0.5$ atm, $P'' < 10^{-8}$ atm) than that during the oxygen permeation experiment ($P' = 0.5$ atm, $P'' \approx 10^{-4}$ atm). A possible change in the mechanisms of electron-transport (such as from *p*-type to *n*-type) and surface reactions when the BYS membrane surface is exposed to methane also may be responsible for the substantial increase in oxygen permeation rate.

As compared with OCM in the BY25 membrane reactor (Zeng and Lin, 2000b), the BYS membrane reactor gives a higher C_2 yield with similar C_2 selectivity. OCM in the BY25 membrane reactor did not produce CO, while there was about 20% CO in total CO_x products in the BYS membrane reactor. In both membrane reactors the C_2H_4/C_2H_6 ratio follows a similar temperature dependence. The surface of BY25 membrane exposed to the methane stream after about 15 h of OCM reactions contained several nonfluorite structured oxide phases in considerable quantities (Zeng and Lin, 2000b). Figure 9 shows the XRD patterns of BYS membrane before and after about 15 h of OCM reactions in the membrane reactor. As shown, the surfaces of the BYS membranes after OCM maintained essentially the same phase structure. This indicates that the BYS membrane is much more chemically stable than the BY25 membrane at high temperatures under a reducing environment.

Cofeed OCM reaction experiments were also conducted in the same BYS membrane reactor to examine how effective the membrane reactor improves the C_2 selectivity of the OCM reactions. In these cofeed experiments CH_4 and O_2, diluted with helium, were cofed into the reaction chamber of the membrane reactor and only N_2 was introduced into the other chamber of the reactor. The feed containing 10% methane was fed into the reaction chamber at total flow rate of 150 mL/min. For comparison on the same basis, C_2 yields for the reactions in both the cofeed and membrane reactor modes were controlled at 3–12%. The results are given in Figures 10 and 11. As shown, the C_2 selectivities in the membrane reactor mode are generally higher than 60%, while those in the cofeed mode are less than 40%.

Table 2 compares the OCM performance in the disk-shaped dense membrane reactor under similar conditions reported in the literature and this work. Two types of oxygen-conducting membranes, perovskite-type and fluorite-type, were used in these studies. The dimensions of these membranes were 15–22 mm in diameter and 1–2.5 mm in thickness. The optimal temperatures were all around 850°C. Except for the study of Xu and Thomson (1997), methane was diluted with helium. The feed velocities in the reaction chamber were among

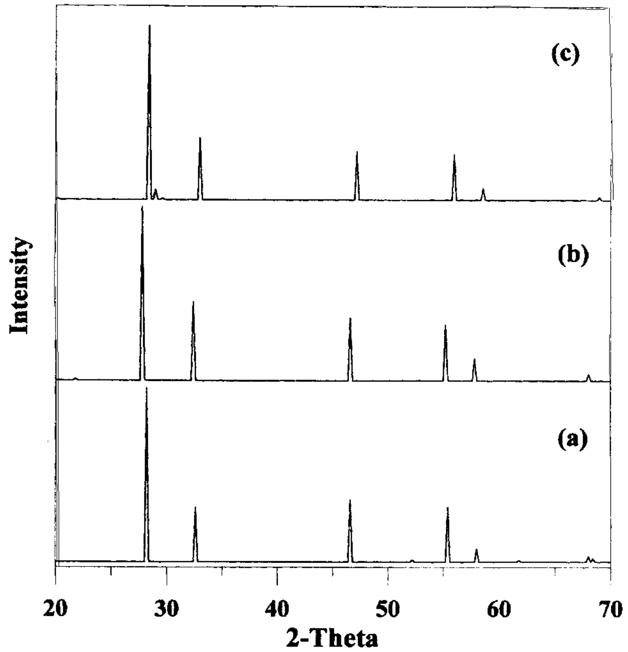

Figure 9. XRD patterns of BYS membrane: (a) before OCM reactions; and after OCM reactions on the surface exposed to (b) O_2; and (c) CH_4.

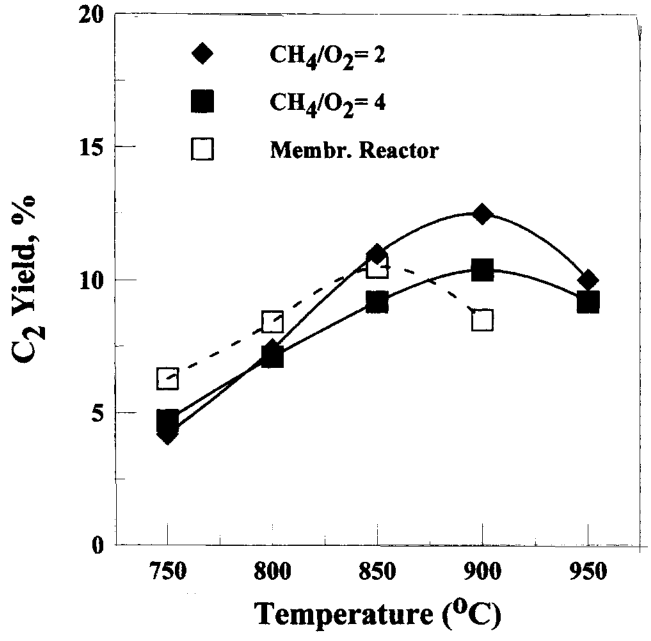

Figure 10. C_2 yields for OCM in the cofeed fixed-bed reactor packed with BYS pellets and those in the BYS membrane reactor.

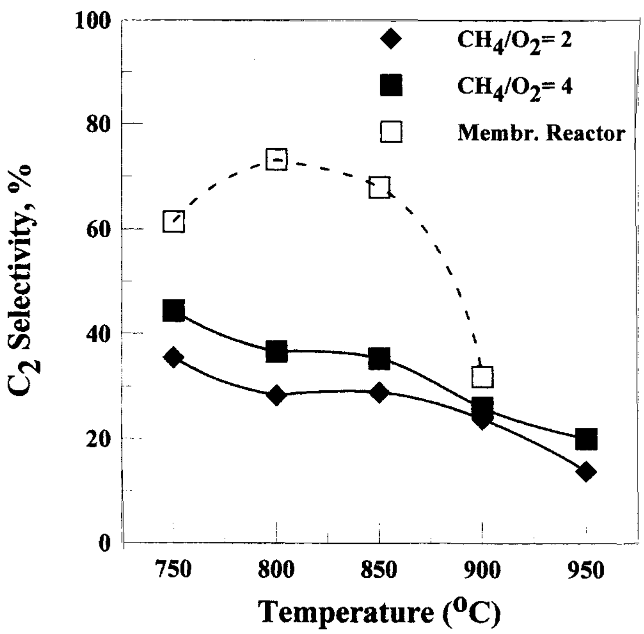

Figure 11. C_2 yields for OCM in the cofeed fixed-bed reactor packed with BYS pellets and those in the BYS membrane reactor.

1.66×10^{-5} to 8.43×10^{-3} mol/s·cm^2. As shown in Table 2, the membrane reactors made of perovskite materials had lower C_2 selectivity than those made of fluorite-type Bi_2O_3-based materials. Substitution of Sr with Ba in the A-site enhanced C_2 selectivity of perovskite-type materials. The lowest C_2 formation rate and oxygen permeation flux was reported by ten Elshof et al. (1995). This could be due to the fact that the feed velocity they used was more than 100 times faster than others; thus, methane residence time was more than 100 times shorter than others. They also found that the oxygen conversion was only 43.8% as compared with 100% in other studies.

The C_2 yields achieved in this work are much higher than those reported in the previous studies on OCM in the disk-shaped dense ceramic membrane reactors (with the membrane surface as the active surface) (Nozaki et al., 1992, 1993, 1994; ten Elshof et al. 1995; Xu and Thomson, 1997; Zeng et al., 1998) (also see Table 2). This is consistent with the extremely high OCM reactivity of the fluorite-structured Bi_2O_3-based ceramics discovered in our previous study in a conventional packed-bed reactor (Zeng and Lin, 1997a). However, the C_2 yield in the current BYS membrane reactor is not as high as expected. This could be explained by a closer look at the reactor configuration.

As shown in Figure 1a, the experiments presented earlier were performed with a feed of O_2/N_2 mixture flowed upward into the 1-in.-OD alumina tube and methane/helium mixture introduced into the 1.5-in.-OD (38 mm) alumina tube. Both streams were introduced into the reaction chambers through the 1/4-in.-OD (6 mm) alumina tubes. The down end of the 1/4-in.-OD tube for the methane stream was placed as close as possible to the membrane surface (such as 0.5 mm in this work). With such a configuration, the reactor had an ineffective gas-phase reaction volume (within the effective heating zone) as large as 108 cm^3, and a membrane surface area as low as 3.14 cm^2. The membrane surface area to gas-phase reactor volume (A/V) ratio was as low as 0.029 cm^{-1}. This A/V ratio is much smaller than that of a fixed-bed reactor packed with dense BYS pellets 1–3 mm in size, which is about 60 cm^{-1}.

The bismuth oxide is extremely active for OCM, with a turnover-frequency for OCM in the range of 140–625 1/s at 900°C (Zeng and Lin, 2000b). Nevertheless, it is possible that the ineffective gas-phase reaction volume in the present membrane reactor configuration is so large that much of methane fed into the reactor would not have the chance to interact with the active oxygen on the membrane surface. This would lower the overall conversion of the reaction. Furthermore, the large ineffective volume would also promote complete combustion reactions with oxygen not consumed for the generation of methyl radicals on the membrane surface. This would also reduce the overall selectivity of the reaction.

Table 2. Comparison of OCM in Disk-Shaped Dense Membrane Reactors under Similar Conditions

	Ten Elshof et al. (1995)	Xu and Thomson (1997)	Zeng et al. (1998)	Zeng and Lin (2000b)	This Work
Membrane material*	Perovksite: LSCF-6482	Perovskite: LBCF-2828	Perovksite: LSCF-8264	Fluorite: BY25	Fluorite: BYS
Membrane dimension (diameter × thickness, mm)	15.2 × 1	17 × 2.5	21.8 × 1.85	21 × 1.4	21 × 1.27
Reaction surface area (cm^2)	1.81	2.27	3.73	3.46	3.46
Reaction temperature (°C)	880	825	850	850	850
Feed flow rate (reaction chamber) (mol/s·cm^2)	8.43×10^{-3}	1.66×10^{-5}	3.59×10^{-5}	2.37×10^{-5}	3.23×10^{-5}
CH_4 in the feed (%)	15	100	4.7	10	10
Feed pressure (atm)	1	1	1	1	1
P_{O_2} in oxygen chamber (atm)	0.21	1	0.5	0.5	0.5
Methane conversion (%)	2.6	2.17	23.7	7.55	15
C_2 Yield (%)	1.17	1.08	8.6	4.05	10.4
C_2 Selectivity (%)	44.9	50	36.2	53	69
C_2H_4/C_2H_6 ratio	0.49	0.43	0.56	1.15	1.1
C_2 formation rate (mol/s·cm^2)	7.38×10^{-9}	9×10^{-8}	7.26×10^{-8}	4.8×10^{-8}	1.68×10^{-7}
O_2 permeation flux (mol/s·cm^2)	8.83×10^{-8}	3.5×10^{-7}	2.1×10^{-7}	2.26×10^{-7}	4.28×10^{-7}

*LSCF and LBSF mean $La_aSr_bCo_cFe_dO_{3-\delta}$ and $La_aBa_bCo_cFe_dO_{3-\delta}$ with the numbers followed indicate the stoichiometric cofficients (such as 6482 represents $a = 0.6$, $b = 0.4$, $c = 0.8$ and $d = 0.2$); BY25 means 25 mol % Y_2O_3 doped Bi_2O_3.

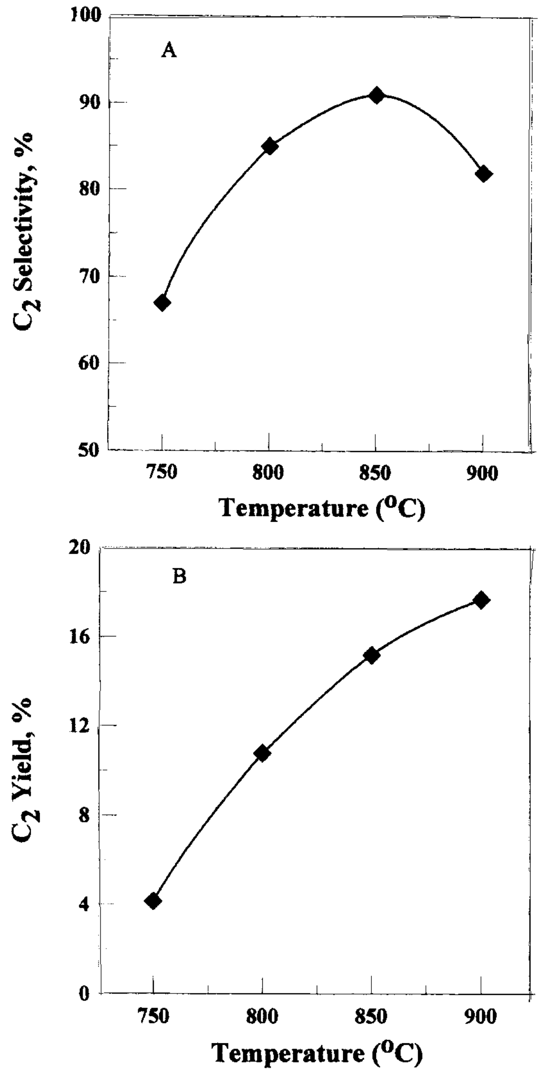

Figure 12. C_2 yield and selectivity as a function of temperature in BYS membrane reactor after modification.

To confirm how the A/V ratio affects the OCM performance in the membrane reactor, the OCM experiments were performed in the same membrane reactor but with a different flow configuration, as shown in Figure 1b. In the modified configuration, oxygen was introduced into the 1.5-in.-OD tube, while methane was fed into the 1-in.-OD tube packed with the inert quartz particles of about 1 mm diameter. After the modification, the A/V ratio for the reaction (based on heating zone) increased about nine times to 0.24 cm^{-1}.

Figure 12 presents the OCM performance in the BYS membrane reactor with the configuration shown in Figure 1b and the feed of 10% methane/helium at 150 mL/min. As shown, C_2 selectivity increases from 65% to about 90%, with the temperature increasing from 750°C to 850°C, and then drops to 80% as the temperature further increases to 900°C. The high C_2 selectivity achieved in the modified reactor suggests that less ethylene was further oxidized into CO_2 as more methane had the chance to come into contact with the membrane surface. Meanwhile, C_2 yield increases dramatically as shown in Figure 12. The highest C_2 yield is 17% at 900°C, comparable to that obtained in a packed-bed reactor. But at this yield the BYS membrane reactor gives much higher C_2 selectivity (about 80%) than the fixed-bed reactor (about 60%). These results indicate that the increase in the A/V ratio of a membrane reactor is indeed effective in improving the performance of OCM reaction in the membrane reactor. One obvious direction to further improve the performance of this new membrane reactor is to change the membrane configuration from disk-shape to the tubular one, as in the latter case the A/V ratio is inversely proportional to the tube diameter.

Conclusions

Oxygen permeation through the BYS membrane is controlled by both surface reactions and bulk electron–hole conduction in 750–950°C with an apparent activation energy for oxygen permeation of about 100 kJ/mol. A much higher C_2 selectivity (> 60%) for OCM can be obtained in the disk-shaped BYS membrane reactor, with the methane and oxygen streams being fed separately into the two reactor chambers (membrane reactor mode), as compared to the case with both streams being cofed to one chamber of the reactor (cofeed mode). The OCM reaction performance of this membrane reactor is related to the oxygen permeation properties of the BYS membrane. With an improved configuration, the disk-shaped membrane reactor gives a C_2 yield as high as 17% with a C_2 selectivity of about 80% for OCM. These results clearly show that a membrane reactor consisting of a highly oxygen permeable ionic conducting ceramic membrane with good OCM catalytic properties can be used to mechanistically manipulate the OCM reactions to improve their product selectivity and yield.

Acknowledgment

The authors acknowledge the support of the NSF (CTS-9502437) on this project.

Literature Cited

Bouwmeester, H. J. M., and A. J. Burggraaf, "Dense Ceramic Membranes for Oxygen Separation," *Fundamentals of Inorganic Membrane Science and Technology*, A. J. Burggraaf and L. Cot, eds., Elsevier, Amsterdam, p. 435 (1996).

Bouwmeester, H. J. M., H. Kruidhof, A. J. Burggraaf, and P. J. Gellings, "Oxygen Permeability of Erbia-Stabilized Bismuth Oxide," *Solid State Ionics*, **53–56**, 460 (1992).

Coronas, J., M. Menendez, and J. Santamaria, "Development of Ceramic Membrane Reactors with a Non-uniform Permeation Pattern," *Chem. Eng. Sci.*, **49**, 2015 (1994).

Fox, J. M., "The Different Catalytic Routes for Methane Valorization: An Assessment of Processes for Liquid Fuels," *Catal. Rev.—Sci. Eng.*, **35**, 169 (1993).

Ito, T., J. X. Wang, C. H. Lin, and J. H. Lunsford, "Oxidative Dimerization of Methane Over a Lithium-Promoted Magnesium Oxide Catalyst," *J. Amer. Chem. Soc.*, **107**, 5602 (1985).

Jiang, Y., I. V. Yentekakis, and C. G. Vayenas, "Methane to Ethylene with 85 Percent Yield in a Gas Recycle Electrocatalytic Reactor Separator," *Science*, **264**, 1563 (1994).

Kao, Y. K., L. Lei, and Y. S. Lin, "A Comparative Simulation Study on Oxidative Coupling of Methane in Fixed-Bed and Membrane Reactors," *Ind. Eng. Chem. Res.*, **36**, 3583 (1997).

Lafarga, D., J. Santamaria, and M. Menendez, "Methane Oxidative Coupling Using Porous Ceramic Membrane Reactors—I. Reactor Development," *Chem. Eng. Sci.*, **49**, 2005 (1994).

Lin, Y. S., W. Wang, and J. Han, "Oxygen Permeation Through Dense Mixed-Conducting Oxide Membranes," *AIChE J.*, **40**, 786 (1994).

Lin, Y. S., and Y. Zeng, "Catalytic Properties of Oxygen Semipermeable Perovskite-Type Ceramic Membrane Materials for Oxidative Coupling of Methane," *J. Catal.*, **164**, 220 (1996).

Lu, Y. P., A. G. Dixon, W. R. Moser, and Y. H. Ma, "Analysis and Optimization of Cross-Flow Reactors for Oxidative Coupling of Methane," *Ind. Eng. Chem. Res.*, **36**, 559 (1997).

Lu, Y. P., A. G. Dixon, W. R. Moser, Y. H. Ma, and U. Balachandran, "Oxidative Coupling of Methane Using Oxygen-Permeable Dense Membrane Reactors," *Catal. Today*, **56**, 297 (2000).

Nozaki, T., O. Yamazaki, K. Omata, and K. Fujimoto, "Selective Oxidative Coupling of Methane with Membrane Reactor," *Chem. Eng. Sci.*, **47**, 2945 (1992).

Nozaki, T., S. Hashimoto, K. Omata, and K. Fujimoto, "Oxidative Coupling of Methane with Membrane Reactor Containing Lead Oxide," *Ind. Eng. Chem. Res.*, **32**, 1174 (1993).

Nozaki, T., and K. Fujimoto, "Oxide Ion Transport for Selective Oxidation of Methane with Membrane Reactor," *AIChE J.*, **40**, 870 (1994).

Ramachandra, A. M., Y. Lu, Y. H. Ma, W. R. Moser, and A. G. Dixon, "Oxidative Coupling of Methane in Porous Vycor Membrane Reactors," *J. Memb. Sci.*, **116**, 253 (1996)

ten Elshof, J. E., H. J. M. Bouwmeester, and H. Verweeij, "Oxidative Coupling of Methane in a Mixed-Conducting Perovskite Membrane Reactor," *Appl. Catal. A*, **130**, 195 (1995).

Tonkovich, A. L., R. W. Carr, and R. Aris, "Enhanced C_2 Yields from Methane Oxidative Coupling by Means of a Separative Chemical Reactor," *Science*, **262**, 221 (1993).

Tonkovich, A. L., and R. W. Carr, "A Simulated Countercurrent Moving-Bed Chromatographic Reactor for the Oxidative Coupling of Methane—Experimental Results," *Chem. Eng. Sci.*, **49**, 4647 (1994).

Tonkovich, A. L. Y., D. M. Jimenez, J. L. Zilka, and G. L. Roberts, "Inorganic Membrane Reactors for the Oxidative Coupling of Methane," *Chem. Eng. Sci.*, **51**, 3051 (1996).

Wang, W., and Y. S. Lin, "Analysis of Oxidative Coupling of Methane in Dense Oxide Membrane Reactor," *J. Memb. Sci.*, **103**, 219 (1995).

Xu, S. J., and W. J. Thomson, "Perovksite-Type Oxide Membranes for the Oxidative Coupling of Methane," *AIChE J.*, **43**, 2731 (1997).

Zeng, Y., and Y. S. Lin, "Catalytic Properties of Yttria Doped Bismuth Oxide Ceramics for Oxidative Coupling of Methane," *Appl. Catal. A*, **159**, 101 (1997a).

Zeng, Y., and Y. S. Lin, "Oxidative Coupling of Methane on Oxygen Semipermeable Yttria Doped Bismuth Oxide Ceramics in Reducing Atmosphere," *Ind. Eng. Chem. Res.*, **36**, 277 (1997b).

Zeng, Y., Y. S. Lin, and S. L. Swartz, "Perovskite Type Ceramic Membranes: Synthesis, Oxygen Permeation and Membrane Reactor Performance for Oxidative Coupling of Methane," *J. Memb. Sci.*, **150**, 87 (1998).

Zeng, Y., and Y. S. Lin, "Synthesis and Properties of Copper and Samarium Doped Yttria-Bismuth Oxide Powders and Membranes," *J. Mater. Sci.* in press (2000a).

Zeng, Y., and Y. S. Lin, "Oxygen Permeation and Oxidative Coupling of Methane in Yttria Doped Bismuth Oxide Membrane Reactor," *J. Catal.*, **193**, 58 (2000b).

Manuscript received April 10, 2000, and Aug. 25, 2000.